The mass-flux approach to the parametrization of deep convection
March 1997

By **D. Gregory**

Table of contents

1. INTRODUCTION

Although the principles of the mass-flux approach to convection were formulated in the 1970s and formed the basis for the well known "Arakawa–Schubert" scheme (Arakawa and Schubert 1974) it has only been recently that such schemes have been used in many GCMs due to their expense compared to simpler schemes (moist convective adjustment and Kuo-type schemes). The approach has a stronger physical basis than these earlier methods and provides an understanding of how convection affects the large-scale atmosphere. It also allows more physically based microphysical treatments to be employed and vertical transports of tracers by convection to be estimated, of importance when considering the impact that aerosols have upon climate.

This paper will outline the mass-flux approach to the parametrization of convection, concentrating "bulk" type schemes such as those used in the ECMWF forecast model (Tiedtke 1989) and the UK Met. Office Unified Model (Gregory and Rowntree 1990). Important issues relating to this approach are discussed by reference to the Tiedtke scheme at ECMWF, although reference is made to other schemes as appropriate. Only brief comments are made concerning the more complex "spectral" cloud model approach, of which the Arakawa–Schubert scheme is the best known example.

2. THE NEED FOR PARAMETRIZATION.

Within large-scale models of the atmosphere the horizontal length scale on which the convection exists is below the resolution used, and so the effects of such clouds must be parametrized in terms of the large-scale flow. Expressing the temperature structure of the atmosphere in terms of a large-scale mean and an unresolved eddy contribution,

$$\phi = \bar{\phi} + \phi' \tag{1}$$

the thermodynamic equation of the large-scale flow may be written as,

$$\frac{\partial \theta}{\partial t} + \overline{\nabla \cdot \mathbf{v}\theta} + \frac{\partial (\overline{\omega}\bar{\theta})}{\partial p} = \frac{L\overline{Q}}{c_p \Pi} + \frac{\partial (\overline{\omega'\theta'})}{\partial p} - Q_R = Q1 - Q_R \tag{2}$$

where Q_R is the radiative heating rate and $Q1$ is termed the apparent convective heat source (Yanai et al. 1973). The left-hand side contains large-scale terms only, while the right-hand side of Eq. (2) represents the impact of radiation and small-scale motions upon the large-scale flow. Convection is seen to affect the large-scale flow through condensational heating and the vertical transport of heat. A similar treatment is applicable to the moisture equation leading to the definition of $Q2$, the apparent moisture sink due to convection and also the horizontal momentum equation, defining $Q3$, the impact of convection upon horizontal momentum.

3. MASS-FLUX THEORY OF CONVECTION

The mass-flux approach was first formulated by Ooyama (1971). It is assumed within some area A, taken to be the grid point of a numerical model, that a fraction σ is covered by cloud. Hence the area average of ϕ is given by

$$\bar{\phi} = \sigma\overline{\phi^c} + (1 - \sigma)\overline{\phi^e} \tag{3}$$

where ϕ^c is the value of ϕ within cloudy air, φ^e that within the environment of the cloud.

It is normally assumed that $\sigma \ll 1$ and so,

$$\bar{\phi} = \bar{\phi}^e \tag{4}$$

Table 1:

σ	ϕ^e	ϕ^c	Error in ϕ^e due to Eq. (4)	Error in B due to Eq. (4)
		Temperature		
0.1	300 K	301 K	< 0.1%	10%
0.5	300 K	301 K	0.2%	50%
		Mixing ratio		
0.1	15 g/kg	17 g/kg	1.3%	
0.5	15 g/kg	17 g/kg	6.5%	

Table 1 provides an indication of the magnitude of the error in the environmental temperature and mixing ratio through the use of Eq. (4), together with the impact upon estimation of parcel buoyancy, evaluated as,

$$B = \frac{\bar{\theta}^c - \bar{\theta}^e}{\bar{\theta}^e} \tag{5}$$

Absolute errors are generally small even when σ is large, which may be the case when the grid size is reduced to that found in meso-scale models (on the order of 10–20 km). Thus, the theoretical formulation developed below is fairly accurate. However, errors in buoyancy (a temperature difference) are much larger. As buoyancy is the main driving force for convection this may lead to errors in the estimation of the intensity of convection.

Consider now the eddy flux divergent contribution to $Q1$. From Eq. (1) it can be written that

$$\overline{\omega'\theta'} = \overline{\omega\theta} - \bar{\omega}\bar{\theta} \tag{6}$$

Using Eq. (3) to expand the first term of the r.h.s. of Eq. (6) and ω in the second term, after rearrangement Eq. (6) can be written as

$$\overline{\omega'\theta'} = \sigma[\overline{\omega\theta}^c - \bar{\omega}^c\bar{\theta}] + (1-\sigma)[\omega\bar{\theta}^e - \bar{\omega}^e\bar{\theta}] \tag{7}$$

Using Eq. (4), and assuming the vertical velocity in the environment is much smaller than that within cloudy air so that motions are only weakly correlated with thermodynamic variables, the second term on the r.h.s. of Eq. (7) can be neglected. The vertical eddy flux due to convective motions is then written approximately as

$$\overline{\omega'\theta'} = \sigma[\overline{\omega\theta}^c - \bar{\omega}^c\bar{\theta}] \tag{8}$$

Hence from Eq. (2) $Q1$ can be expressed as,

$$Q1 = (1-\sigma)\frac{L\bar{Q}^e}{c_p\Pi} + \sigma\frac{L\bar{Q}^c}{c_p\Pi} - \frac{\partial}{\partial p}\{\sigma(\overline{\omega\theta}^c - \bar{\omega}^c\bar{\theta})\} \tag{9}$$

The latent-heating term associated with the cloud environment is usually interpreted as the evaporation of cloud condensate and precipitation detrained from the cloud into clear air leading to a cooling of the cloud environment.

From Eq. (9) it is seen that $Q1$ has been expressed in terms of cloud and large-scale variables. The latter are available from the grid-point fields of the numerical model while the former are usually obtained from the use of a model of a convective cloud, typically a one-dimensional steady-state entraining-plume model of the cloud.

Following the analysis of Gregory and Miller (1989), consider the thermodynamic and continuity equation averaged over an individual cloud (denoted by the subscript i);

$$\frac{\partial}{\partial t}(\sigma_i\bar{\theta}_i^c) - \theta_{bi}\frac{\partial\sigma_i}{\partial t} + \sigma_i\left(\overline{\frac{\partial u\theta}{\partial x}}\right)_i^c + \frac{\partial}{\partial p}(\sigma_i\overline{\omega\theta}_i^c) - (\omega\theta)_{bi}\frac{\partial\sigma_i}{\partial p} = \sigma_i\frac{L\bar{Q}^c}{c_p\Pi} \tag{10}$$

$$\sigma_i\left(\overline{\frac{\partial u}{\partial x}}\right)_i^c + \frac{\partial}{\partial p}(\sigma_i\bar{\omega}_i^c) - \omega_{bi}\frac{\partial\bar{\omega}^c}{\partial p} = 0 \tag{11}$$

where the subscript b refers to the value of a variable on the cloud boundary. These equations are too complex to

use in a scheme and it is usual to approximate the horizontal advection across the cloud boundary, the fluxes across the cloud boundary as it varies with height and the horizontal growth of the cloud with time by entrainment and detrainment fluxes;

$$\frac{\partial}{\partial t}(\sigma_i \bar{\theta}_i^c) - E_i \bar{\theta} + D_i \bar{\theta}^c + \frac{\partial}{\partial p}(\sigma_i \overline{\omega \theta}_i^c) = \sigma_i \frac{L \bar{Q}^c}{c_p \Pi} \tag{12}$$

$$-E_i + D_i + \frac{\partial}{\partial p}(\sigma_i \bar{\omega}_i^c) = -\frac{\partial \sigma_i}{\partial t} \tag{13}$$

where E is the entrainment rate (the rate at which air is included into the cloud through its sides to balance the increase of vertical mass flux in the cloud with height), and D the detrainment rate (the rate at which air leaves the cloud as the cloud vertical mass flux decreases with height). These are defined as

$$E_i = \frac{\partial}{\partial p}(\sigma_i \bar{\omega}_i^c) + \frac{\partial \sigma_i}{\partial t} \quad \text{if} \quad -\frac{\partial}{\partial p}(\sigma_i \bar{\omega}_i^c) - \frac{\partial \sigma_i}{\partial t} < 0$$

$$D_i = \frac{\partial}{\partial p}(\sigma_i \bar{\omega}_i^c) + \frac{\partial \sigma_i}{\partial t} \quad \text{if} \quad -\frac{\partial}{\partial p}(\sigma_i \bar{\omega}_i^c) - \frac{\partial \sigma_i}{\partial t} > 0 \tag{14}$$

These equations are for one cloud only, whereas in the area under consideration it is assumed that there are many clouds. Summing over all cloud within the ensemble, Eqs. (12) and (13) can be written as,

$$-E \bar{\theta} + \sum_{\text{det}} D_i \bar{\theta}^c + \frac{\partial}{\partial p}(\sigma \overline{\omega \theta}^c) = \sigma \frac{L \bar{Q}^c}{c_p \Pi} \tag{15}$$

$$-E + D + \frac{\partial}{\partial p}(\sigma \bar{\omega}^c) = 0 \tag{16}$$

where $E = \sum E_i$ and $D = \sum D_i$, the summation being carried out over all clouds. The summation on the l.h.s of Eq. (15) is over all clouds which are undergoing terminal detrainment. It has also been assumed that the whole ensemble is in a steady state, and so remaining time dependent terms can be neglected.

Substitution of Eqs. (15) and (16) into Eq. (9) gives, after rearrangement,

$$Q1 = \sigma \bar{\omega}^c \frac{\partial \bar{\theta}}{\partial p} + \sum_{\text{det}} D_i(\bar{\theta}_i^c - \bar{\theta}) + (1 - \sigma)\frac{L \bar{Q}^e}{c_p \Pi} \tag{17}$$

A similar analysis can be applied to the moisture equation to obtain $Q2$ and the horizontal momentum equation to give $Q3$.

Convection modifies the large-scale atmosphere through;

(a) *compensating subsidence*—motion in the clear environment surrounding the cloud compensating motion within the cloud (a consequence of mass continuity),

(b) *detrainment of cloudy air into the environment*,

(c) *the evaporation of cloud condensate and precipitation within the environment*—either through detrainment or below cloud base as precipitation falls to the surface. This later term is closely tied

to microphysical processes and, because of the fall-out of precipitation, is not uniquely related to the mass-flux and condensation profiles within the convection.

4. EVALUATION OF MASS-FLUX THEORY

Several authors have attempted to diagnose the magnitude of the terms in Eq. (17) using observations (e.g Yanai *et al.* 1973). However this method relies on using simple cloud models, identical to those used in parametrization schemes, to estimate in-cloud variables. The technique is essentially using a convective parametrization in a diagnostic mode. More recently diagnostics from cloud-resolving models have helped to understand the mass-flux approach (e.g. Gregory and Miller 1989). Fig. 1 from the latter study (a simulation of convection during phase 3 of GATE) compares the vertical structure of $Q1$ with that of compensating subsidence and the evaporation of condensate within the cloud environment. Compensating subsidence is seen to follow $Q1$ closely in the vertical, exceeding it at most levels. This excess of heating is compensated by the evaporation term. The detrainment of cloudy air plays only a secondary role for deep convection, although it is of greater importance in shallow convection (see Soong and Ogura 1980). These results agree with studies using observational data, for example that of Yanai et al. (1973) using data from the west Pacific.
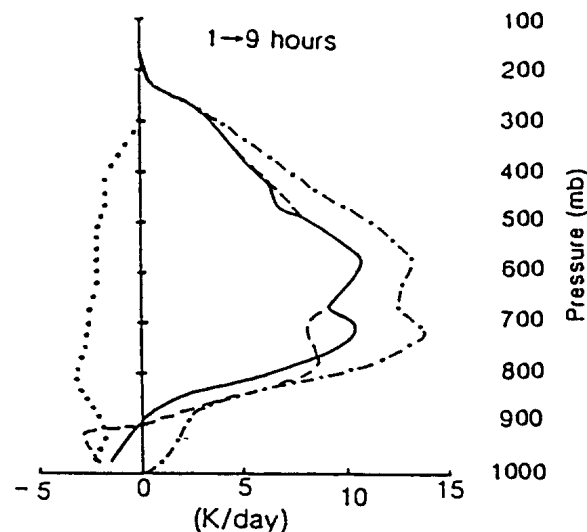
Figure 1. Profile of compensating subsidence (dot-dash), evaporation of cloud and precipitation (dotted), their sum (solid) and net Q1 (dashed) for convection in a phase III GATE easterly wave (From Gregory and Miller 1989).

However for $Q2$, Gregory and Miller (1989) suggest that a combination of compensating subsidence and the evaporation of condensate within the cloud environment is not a good approximation (Fig. 2), drying at 800 mb being overestimated by this approximation and underestimated below this level. This is a consequence of several factors. Firstly above 800 mb detrainment plays a much larger role in the moisture budget than for temperature (see also the recent study by Guichard et al. (1996)). As the air detrained from convection is saturated, its mixing ratio is usually further away from the environmental value than is the case for temperature, and so detrainment has a much larger impact in the moisture budget than in the corresponding heat budget. This was also noted in earlier observational studies. In the lowest 200 mb of the domain the difference is partially caused by the inability of the coarse-resolution model to simulate shallow convection, but also by the fact that "entrainment" into the lower part of the cloud dries the domain. This is due to the environment around the base of the convection being wetter than the

average across the domain, implying that the large-scale average value of mixing ratio is a poor representation of air flowing into convection near cloud base. This effect is not usually accounted for in parametrization schemes. In general the moisture errors found in GCMs in convective regions are larger than those for temperature, partially a consequence of poor formulation of the entrainment and detrainment processes for moisture used in current schemes.
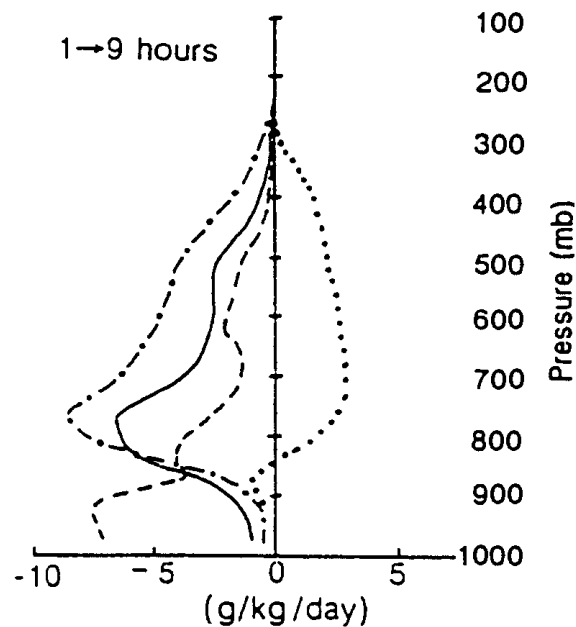
Figure 2. Profile of compensating subsidence (dot-dash), evaporation of cloud and precipitation (dotted), their sum (solid) and net Q2 (dash) for convection in a phase III GATE easterly wave (From Gregory and Miller 1989).

Cloud resolving models allow the contribution of updraughts and downdraughts to the net convective heating and drying to be determined. Fig. 3 shows $Q1$ due to updraughts and downdraughts for the GATE simulation of Gregory and Miller (1989). The heating due to updraughts is twice $Q1$, the excess heating being compensated by the cooling due to the evaporation of precipitation with downdraughts. Such a large contribution to the net heating implies that it is important to include downdraught processes in convective parametrizations. Similar conclusions have also been reached from observational studies (e.g. Betts 1973).
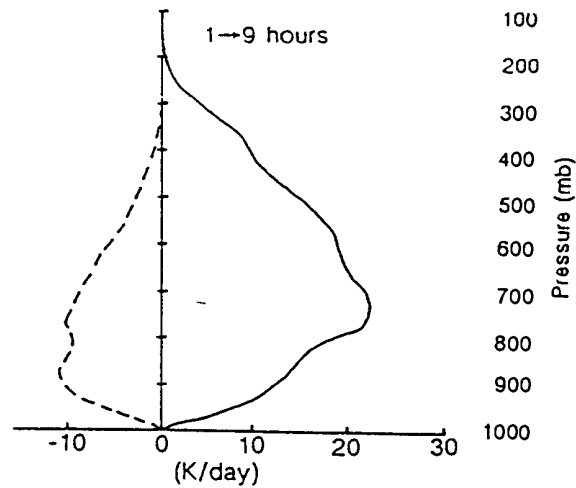
Figure 3. Contribution of updraughts (solid) and downdraughts (dashed) to Q1 for convection in a phase III GATE easterly wave (From Gregory and Miller 1989).

5. PRACTICAL APPLICATION OF MASS-FLUX THEORY

Application of the above theory in a numerical model is a two-stage process. Firstly a cloud model must be used to estimate the vertical distribution of the cloudy quantities, and secondly the magnitude of the mass flux at the base of the cloud must be determined, usually by some reference to the large-scale structure and forcing (the closure problem).

5.1 Estimation of cloud properties

Two approaches are commonly to estimate the quantities required to implement the mass-flux theory as a parametrization scheme. The first approach uses a spectral cloud ensemble, in which several different cloud models are used to represent differing cloud types within a grid box of a GCM. In the second approach, the bulk cloud-model method, a single cloud model is used to represent an ensemble of clouds. The strengths and weaknesses of each approach are discussed below.

5.1 (a) Spectral cloud ensemble approach. This technique was first introduced by Arakawa and Schubert (1974). They assumed that within a grid box of a GCM a spectrum of different height clouds existed. Each cloud is characterised by a different entrainment rate, and so a different cloud top height (Fig. 4). Clouds with large entrainment rates terminate lower in the atmosphere (cloud 1), while those with lower entrainment rates follow a more undiluted ascent, and so terminate in the upper troposphere (cloud 3). In theory, the number of different cloud types within the distribution is arbitrary with clouds allowed to terminate at any level in the atmosphere, but in practice the number of cloud types is limited by the number of vertical levels in the model, one cloud type detraining at each model layer.
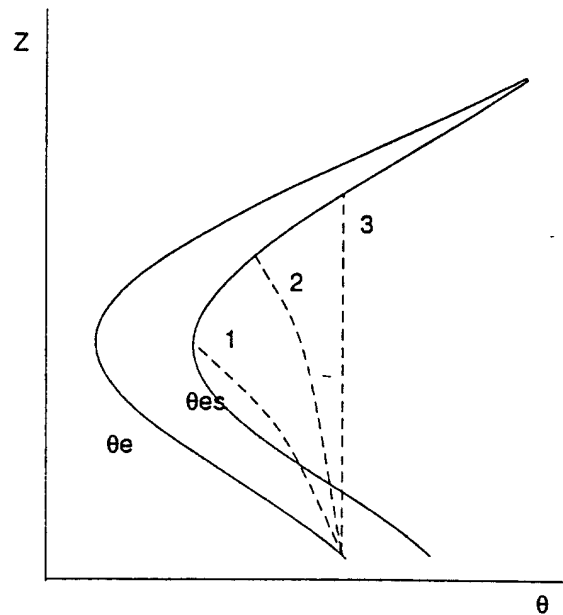
Figure 4. Schematic of spectral cloud ensemble approach. Curves 1,2 and 3 represent ascent of air in clouds with differing entrainment rates.

The cloud-base mass flux must be estimated for each cloud type (the "closure problem"), determining how much that cloud type contributes to the ensemble mean. The original version of the Arakawa–Schubert scheme required an iterative solution to solve for the distribution of mass flux associated with each cloud type, but in recent years the scheme has undergone some modification (e.g. Moorthi and Suarez 1992) in order to reduce its complexity and increase its robustness, while still retaining the spectral cloud-ensemble approach.

5.1 (b) Bulk cloud model approach. Because of the complexity (and hence the computational expense) of the spectral cloud-ensemble approach, several schemes have been developed using the simpler bulk-cloud model approach suggested by Yanai et al. (1973). In this method, only one cloud model is used to represent an ensemble of clouds within a grid box, the cloud properties predicted being averages over the cloud ensemble whose members have ascents ranging from cloud type 1 to cloud type 3 (Fig. 5). Both the mass-flux scheme of Tiedtke (1989) used in the ECMWF model, and the UK Meteorological Office scheme (Gregory and Rowntree 1990), use this approach. The approach has also been used in meso-scale models (e.g. Fritsch and Chappel 1980) where, due to smaller grid sizes, it is reasonable to assume that only one cloud type exists within a grid box. The method is cheaper and simpler to implement, and both of these schemes have the additional advantage over the Arakawa–Schubert scheme that they are able to represent convection that is not rooted in the planetary boundary layer (for example as seen in mid-latitude warm fronts).
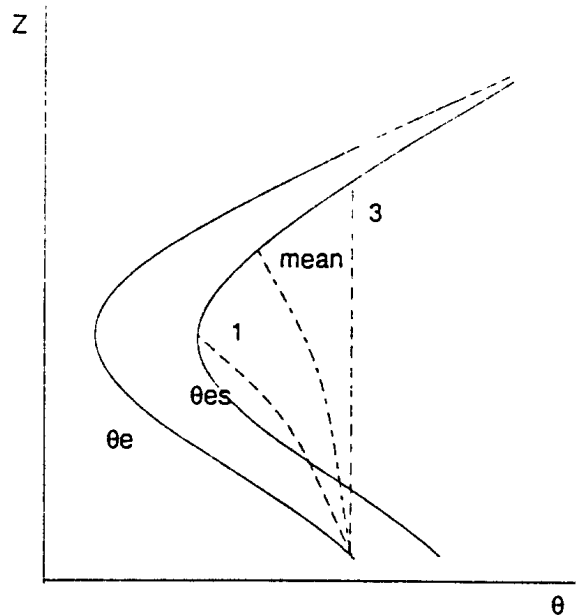
Figure 5. Schematic of bulk-cloud approach. Mean curve represents the ascent of air in the "bulk" cloud
representing a mean over an ensemble of ascents ranging from ascent 1 through 3.

5.2 Issues in the formulation of bulk mass-flux schemes

Here discussion of the mass-flux approach is focused upon issues relating to the bulk cloud-model approach. The
Tiedtke scheme, used in the ECMWF model, is used to illustrate issues which must be addresses in designing such
a scheme.

5.2 (a) Determination of cloud type. In the spectral cloud model approach, several cloud types with differing
lateral mixing rates and cloud-top heights are present within each grid box, the "closure method" determines the
fraction of the total mass flux associated with each cloud. Thus, in theory, the method is able to distinguish the
type of convection in a variety of regimes. In the tropics the ensemble would be dominated by deep convection,
while in the subtropical trade-wind regions shallow convective cloud would dominate the ensemble. When using
a bulk scheme, only one cloud type is present in each grid box of a model and so some a priori decision must be
made as to the type of convection present, allowing the lateral mixing properties and the estimation of cloud-base
mass flux to be varied depending upon whether the convection is dominated by deep or shallow convection. For
example, shallow convection is smaller and more turbulent that deep convection and so will have a higher entrain-
ment rate than deep convection.

Such "switching" is usually done on the basis of an aspect of the large-scale environment in which the convection
is growing. For example, observations show that deep convection is often collocated with regions of moisture con-
vergence, while shallow convection is found to occur under low-level inversions caused by large-scale subsidence,
where the moisture supply to the planetary boundary layer is dominated by evaporation from the surface. Thus in
the Tiedtke scheme used at ECMWF, if the large-scale convergence of moisture into a column is larger than the
surface evaporation then convection is deemed to be deep and a low entrainment rate set for the purpose of estimat-
ing the ascent of a parcel, and hence its in-cloud properties. If the converse is so, then higher entrainment rates are
set appropriate to shallow convection (being four times larger than those used for deep convection).

5.2 (b) Formulation of entrainment and detrainment.   A further issue with the bulk approach is the specification of entrainment and detrainment rates. Simulations made by GCMs show a large degree of sensitivity to these quantities (see paper on "Sensitivity of GCM performance to convective parametrization" and Yao and DelGeno (1989)). Cloud-top height is very sensitive to the magnitude of the entrainment rate. With only one plume present the entrainment rate must be set so as to allow the maximum cloud-top height to be correctly estimated. Also, account has to be taken of those clouds which, in reality, detrain at levels lower than this height. This is usually done by including a background detrainment rate in addition to that which occurs at the top of the plume. For the Tiedtke scheme in cases of deep convection, entrainment is applied below the level of the maxima in large-scale vertical velocity, while a fixed (so-called "mixing") detrainment rate is applied throughout the cloud depth. The depth and magnitude of the terminal detrainment near cloud top is estimated by the decrease in parcel kinetic energy caused by the overshoot of a parcel above its neutral buoyancy level. This ad hoc approach matches the shape of the mass-flux profile with that of the grid-scale motion, generally a feature observed in deep convective regions. In the case of shallow convection the entrainment and mixing detrainment rates are equal and constant with height, implying a constant mass flux above cloud base until the parcel becomes negatively buoyant.

In recent years the validity of the entraining/detraining plume cloud model widely used in mass-flux schemes has been questioned. Raymond and Blyth (1986) studying cumulus clouds suggested that mixing across the cloud boundary occurs episodically rather than continually, with parcels of air that become negatively buoyant on mixing descending to their level of neutral buoyancy before leaving the cloud. Schemes discussed by Kain and Fritsch (1990) and Emanuel (1991) have incorporated simplified versions of this model into convection schemes for use with meso-scale and climate models. Nordeng (1994) has also suggested a revised specification of entrainment rates for the ECMWF convection scheme for use within the frame work of the entrainment/detraining plume approach, with entrainment rates linked to the buoyancy of the parcel.

5.3 Performance of "cloud ensemble" and "bulk schemes"

Although the bulk cloud model approach is simpler than the Arakawa–Schubert scheme, it performs well in both climate and NWP applications. Fig. 6 shows December/January/February precipitation averaged over the 10 years of the AMIP decade (1979–1988) (Slingo et al. 1996) simulated by a version of the ECMWF model (T42, 19 levels) using a version of the Tiedtke scheme and the GLA model ($4° \times 5°$, 11 levels) which employs a version of the Arakawa–Schubert scheme. An observed climatology derived from satellite observations (Spencer 1993), estimated from microwave sounding unit (MSU) data) is also shown. Differences to the climatology are seen but both models give a reasonable estimate of the distribution of precipitation. The ECMWF simulation has stronger precipitation over the west Pacific and the Pacific ITCZ, but underestimates rainfall in the SPCZ. The GLA model overemphasises the SPCZ and underestimates the rainfall north of the equator in the Pacific.
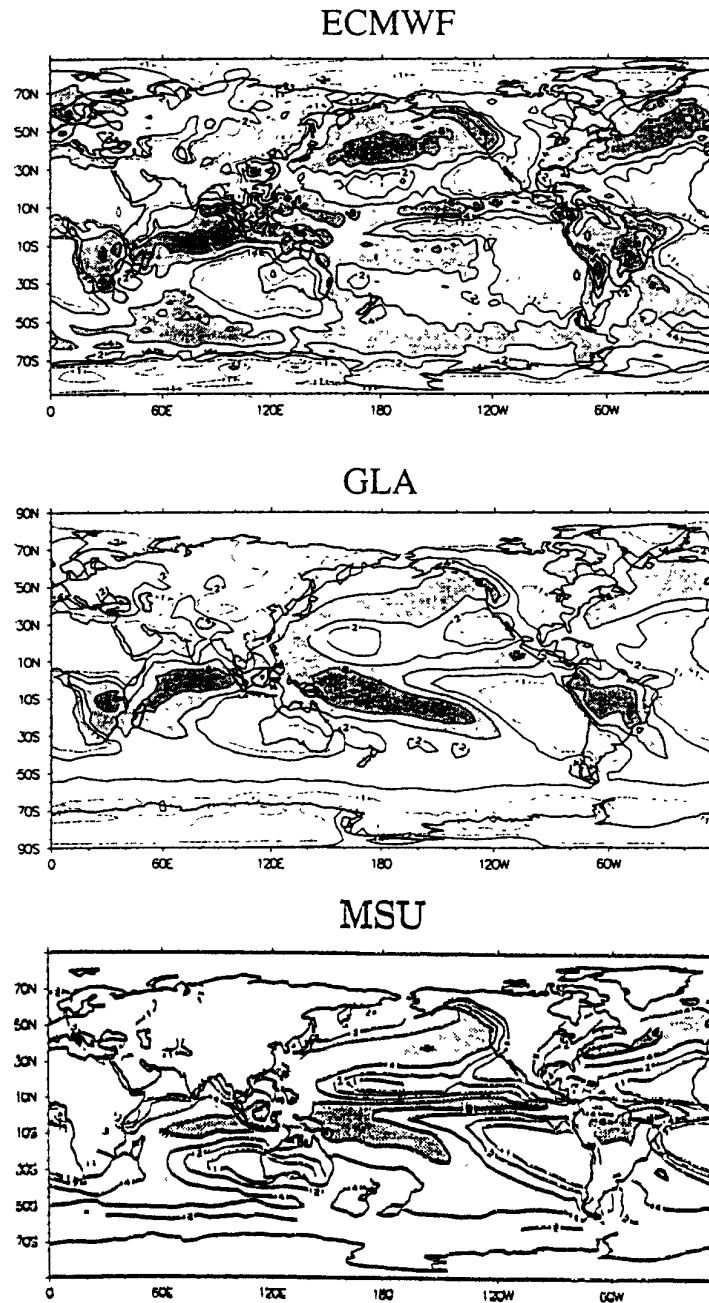
Figure 6. Comparison of DJF precipitation averaged over the AMIP decade (1979–1988) simulated by the ECMWF (T42, 19 levels) and GLA (4 x 5 degrees, 11 levels) GCMs together with a climatogy from Spencer (1993) derived from MSU data (adapted from Slingo *et al*. (1996)).

5.4 Representation of downdraughts

As discussed above, downdraughts play a large role in the convective heat budget. In parametrizations these are usually modelled by an inverted entraining plume starting near the level of minimum equivalent potential temperature in the mid troposphere. The magnitude of the downdraught mass flux has to be determined. Some schemes estimate the activity of the downdraught from empirical relationships between observed precipitation efficiency

and the vertical shear of the horizontal wind (Fritsch and Chappel 1980). In the Tiedtke scheme a simpler approach is used, the initial mass flux at the top of the plume being set to a third of the of the updraught mass flux at cloud base. As air descends it is cooled by the evaporation, maintaining negative buoyancy, and finally detrains into the subcloud layer which it tends to cool and dry. One weakness with current schemes is that they often assume that evaporation of precipitation within the downdraught maintains saturation, whereas observations suggest that they remain unsaturated (Betts 1973). This may cause errors in the subcloud-layer budgets of heat and moisture.

5.5 Estimation of cloud base mass flux

For mass-flux parametrization schemes, the closure problem is essentially the need to estimate the convective mass flux at the base of the cloud. This determines the magnitude of the convective heat release while the cloud model, and associated cloud microphysical parametrization used, determines how this heat is distributed in the vertical. No exact theory exists for the closure problem and several different methods have been used. Howeve, it is possible to broadly classify these various closures into "dynamical" and "adjustment" types.

5.5 (a) Dynamical closure. "Dynamical" closures relate the cloud-base mass flux to the large-scale forcing and atmospheric structure, usually making some assumption regarding the "quasi-equilibrium" of the convecting atmosphere. The closure of the Arakawa and Schubert (1974) scheme is of this type, relating convective activity to large-scale forcing throughout the depth of the convecting layer. The Tiedtke (1989) scheme estimates cloud-base mass flux from an equilibrium assumption on either moisture (for deep convection) or moist static energy (for shallow convection) integrated over the subcloud layer. Such a closure relates to the ideas of boundary-layer quasi-equilibrium put forward by Raymond (1995) .

Integrating over the subcloud layer, and assuming that there is a balance between convection and other processes (surface fluxes, turbulence, large-scale motion), then

$$M_{z_b}^u(q_{z_b}^u - \bar{q}) + M_{z_b}^d(q_{z_b}^d - \bar{q}) \ = \ \int\limits_0^{z_b} \rho F_q \mathrm{d}z \tag{18}$$

where M^u, M^d, q^u and q^d are the updraught and downdraught mass flux and mixing ratios, F_q is the forcing due to surface fluxes, turbulence and large-scale motion and z_b is the height of cloud base. Quantities with the subscript z_b refer to their values at cloud base. As the downdraught mass flux is related to the updraught mass flux at cloud base, Eq. (18) can be rearranged to give an estimate for the cloud-base mass flux.

5.5 (b) Adjustment closure. In schemes which use an "adjustment" closure, the cloud-base mass flux is calculated from relaxing the large-scale atmosphere back to an equilibrium structure. The Fritsch and Chappel (1980) scheme provides an example of this type of closure, where the cloud-base mass flux is calculated from the reduction of Convective Available Potential Energy (CAPE) over a time scale τ .

CAPE is defined as

$$\mathrm{CAPE} \ = \ \int\limits_{\mathrm{cloud}} (\bar{\theta}^c - \bar{\theta}) \, \frac{\mathrm{d}p}{\rho g} \tag{19}$$

(ignoring virtual effects for simplicity).

Assuming steady state clouds, the rate of change of CAPE with time due to convective activity is given by

$$\left(\frac{\partial \mathrm{CAPE}}{\partial t}\right)_{\mathrm{conv}} = -\int g\left(\frac{\partial \bar{\bar{\theta}}}{\partial t}\right)_{\mathrm{conv}}\frac{\mathrm{d}p}{\rho g} = -\int \rho Q 1 \frac{\mathrm{d}p}{\rho g} \qquad (20)$$

Approximating $Q1$ by a subsidence term, and assuming that convection reduces CAPE to zero over a timescale τ, the cloud-base mass flux is given by,

$$m_{\mathrm{B}} = \frac{\mathrm{CAPE}}{\tau}\frac{1}{\int \eta(p)\frac{\partial \bar{\bar{\theta}}}{\partial p}\frac{\mathrm{d}p}{\rho g}} \qquad (21)$$

where $M_{\mathrm{B}}(p)$ is the mass flux i.e. $\eta(p)$ is the mass flux normalised by its value at cloud base.

The time scale for adjustment is resolution dependent due to the magnitude of the resolved vertical velocity on small horizontal scales increasing as resolution decreases (Nordeng 1994). If a quasi-equilibrium is assumed to exist then moistening due to large-scale ascent is approximately balanced by compensating subsidence implying that

$$M_{\mathrm{c}} = \rho \overline{w} \qquad (22)$$

In general, the resolved magnitude of the vertical velocity roughly doubles as the horizontal grid length is halved, implying that the time scale for adjustment must decrease as resolution increases.

6. EVALUATION OF CONVECTION SCHEMES USING CLOUD RESOLVING MODELS

It has already been shown that the bulk mass-flux approach to convective parametrization is able to provide a broadly comparable distribution of global precipitation to that obtained through the use of more complex scheme (Fig. 6). The development of cloud-resolving models with the ability to capture accurately features of convective clouds allows more detailed evaluation of the realism of the representation of convection afforded by the mass-flux approach. Quantities such as updraught and downdraught mass flux are poorly specified by observations but are readily diagnosed from cloud-resolving models, providing a powerful tool to evaluate the assumptions used to generate these key quantities.

Here mass fluxes estimated from the Tiedtke convection scheme in a single-column version of the ECMWF forecast model are compared with those estimated by cloud-resolving models (CRMs) for three different cases;

(a)   tropical convection during GATE. Constant cooling and moistening tendencies representing the effects of large-scale ascent are provided to the model and surface fluxes and sensible and latent heat (12 and 145 W m^{-2}) respectively are held constant

(b)   convection in a cold-air out break forced by surface fluxes only (sensible- and latent-heat fluxes of 123 and 492 W m^{-2}, respectively)

(c)   shallow convection during BOMEX (based upon a case study of Holland and Rasmusson (1973))

Further details of cases (a) and (b) are presented in Kershaw *et al.* (1997) and Gregory *et al.* (1997), while the BOMEX case is discussed by Siebesma and Holtslag (1996). The convection scheme is as used in CY14R3 of the ECMWF model. The closure of the scheme differs from that described above in that only updraught fluxes of moisture out of the boundary layer are considered to balance the forcing in the subcloud layer. This does not affect the average properties of convection over the 10 hour period of experiments (a) and (b), the convection scheme being in balance with the forcing supplied to the model. However the evolution of the convective heating is changed and

this will be illustrated for the GATE case. Case (c) is unaffected by this change as no downdraughts form.

For the GATE case (Fig. 7 : 10 hour average), the depth of the updraught is overestimated implying that the entrainment rates specified may be too low. Updraught mass flux is underestimated by 25% in the lowest 4 km, partially compensated by too weak a downdraught compared with that diagnosed from the CRM. The decrease in mass flux above 5 km is reasonably captured by the detrainment rate specified. The evolution of precipitation for this case is shown in Fig. 8 , where the impact of including the downdraughts into the estimation of cloud-base mass flux is illustrated (Fig. 8 (b)). Without downdraughts (Fig. 8 (a)) the convective response becomes intermittent, the amount of precipitation released in individual convective events being much larger than the moisture supply to the model. Between periods of intense deep convection shallow convection occurs, contributing to the large mass flux at cloud base seen in Fig. 7 .
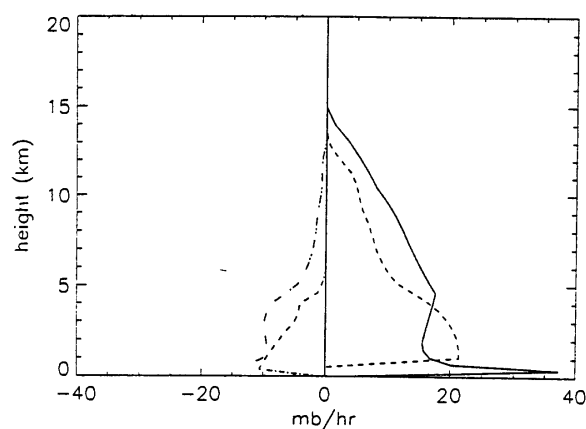
Figure 7. Comparison of convective mass fluxes for updraught and downdraughts predicted by the Tiedtke convection scheme (UD : solid/DD : dot-dash) and diagnosed from a cloud resolving model simulation (UD : dash/ DD : triple dot-dash) for convection in a GATE easterly wave (10-hour averages).

Such behaviour is caused by updraughts balancing the moisture supply in the subcloud layer, leaving downdraughts to dry the layer and so stabilise the profile with respect to deep convection. With downdraughts included the response of the convection is steady, the precipitation amount being in quasi-equilibrium with the moisture supplied to the model. The magnitude of updraught mass flux near cloud base is reduced as deep convection occurs through the entire simulation, although above 2 km the mass-flux structure is similar to that in Fig. 7 .

For the cold-air outbreak case (Fig. 9 : 10 hour average) the moisture convergence into the column is zero, apart from surface evaporation and the switching described above sets the plume parameters to those appropriate to shallow convection even though, from the CRM simulation, it is clear that the convection is deep. With large entrainment rates the depth of convection is underestimated and large detrainment rates cause the mass flux, which is overestimated at the base of the cloud, to fall too rapidly with height. This case points out a deficiency in the switching mechanism used to determine whether convection is deep or shallow. It should be noted that forcing the scheme to use the deep-convective values for entrainment and detrainment produces an updraught mass-flux profile that is in better agreement with that of the CRM.
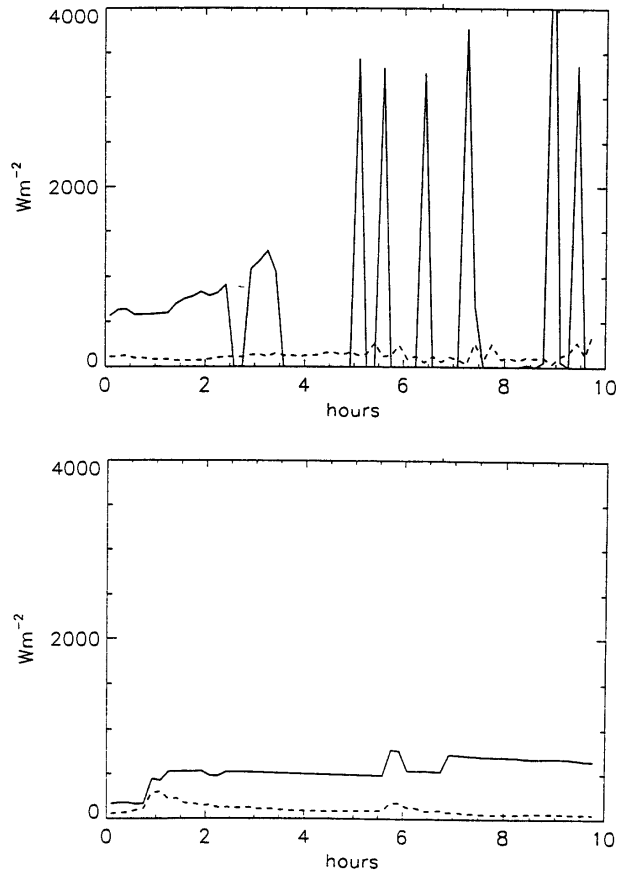
Figure 8. Evolution of rainfall for simulation of convection in GATE given by the Tiedtke convection scheme with closured in which (a) downdraughts are neglected and (b) downdraughts are included into the estimation of cloud base mass flux. Solid curve : convective precipitation. Dashed curve : stratiform precipitation.
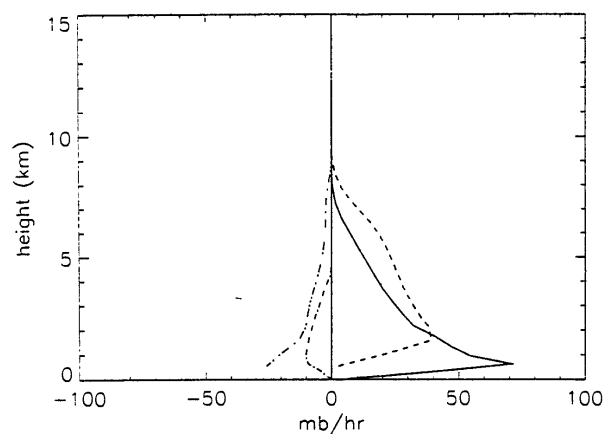
Figure 9. Comparison of convective mass fluxes for updraught and downdraughts predicted by the Tiedtke convection scheme (UD : solid/DD : dot-dash) and diagnosed from a cloud resolving model simulation (UD : dash/ DD : triple dot-dash) for convection in a cold air outbreak (10-hour averages).

The BOMEX case (Fig. 10 : average between 12 and 36 hours) is one in which the large-scale motion above a low-level inversion is downward, and so rightly the convection scheme determines that this is a case of shallow convection. The CRM simulation suggests that mass flux reduced with height across the cloud layer, implying that detrainment rates are larger than entrainment rates. With the Tiedtke scheme the cloud-base mass flux is underestimated and, due to entrainment and detrainment rates being equal, does not changed with height until the inversion layer when an additional "terminal" detrainment occurs as the ascending parcels' vertical kinetic energy decreases. Increasing entrainment rates by a factor of 2 and detrainment rates by a factor of 3, roughly matching those diagnosed from the CRM, gives a larger cloud-base mass flux and a profile that better matches that of the CRM (Fig. 10 : dotted curve). Siebesma and Holtslag (1996) found a similar sensitivity using an earlier version of the Tiedtke convection scheme. With increased entrainment and detrainment rates the thermodynamic structure is also closer to that observed during BOMEX.
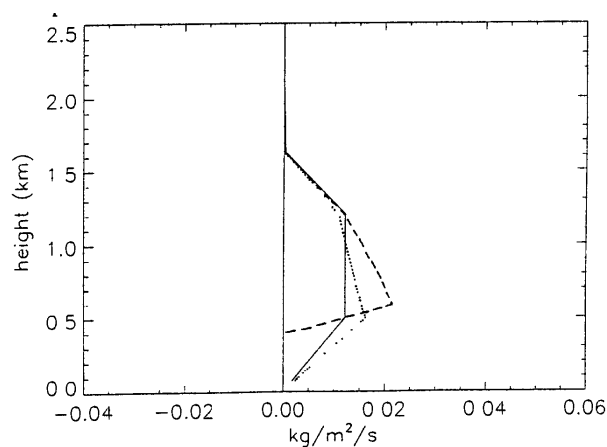
Figure 10. Comparison of updraught mass flux predicted by the standard Tiedtke convection scheme (solid), a version with increased entrainment and detrainment rates (dotted) and diagnosed from a cloud-resolving model simulation (dash) for convection during BOMEX (24-hour averages).

7. CONCLUDING COMMENTS

This paper has outlined the theoretical basis of mass-flux convection schemes and described how this is applied in practice, concentrating upon a class of parametrizations based around the "bulk" cloud model approach of Yanai *et al.* (1973). This method is simpler than the spectral approach, such as in the Arakawa–Schubert scheme, but gives reasonable estimates of global precipitation patterns in GCMs. This type of scheme depends upon correct a priori decisions being made as to the dominant nature of convection at a grid point and its internal characteristics. Using the Tiedtke scheme, the ability of these type of schemes to represent convection in a variety of circumstances has been commented upon through comparison with cloud-resolving model simulations. This identifies areas where modification is required, such as the "switching" criteria to distinguish deep and shallow convective cases, together with the entrainment rates used. Future studies of a variety of convective regimes will be useful to improve the representation of such processes in parametrizations.

REFERENCES

Arakawa, A. and Schubert W.H. (1974) Interaction of a cumulus cloud ensemble with the large-scale environment.

Part I, J. Atm. Sci., 31, 674-701

Betts, A.K. (1973) A composite mesoscale cumulonimbus budget, J. Atm. Sci., 30, 597-610

Emanuel, K.A (1991) A scheme for representing cumulus convection in large-scale models, J. Atmos. Sci., 48, 2313-2335

Fritsch, J.M. and Chappel, C.F. (1980) Numerical prediction of convectively driven mesoscale pressure systems. Part I : Cumulus parametrization, J. Atm. Sci., 37, 1722-1733

Gregory, D. and Miller M.J. (1989) A numerical study of the parametrization of deep tropical convection, QJR. Meteorol. Soc., 115, 1209-1242

Gregory, D. and Rowntree P.R. (1990) A mass flux convection scheme with representation of cloud ensemble characteristics and stability dependent closure, Mon. Wea. Rev., 118, 1483-1506

Gregory, D., Kershaw, R. and Inness, P.M. (1997) Parametrization of momentum transports by convection II : Tests in single column and general circulation models, accepted for publication in QJR. Meteorol. Soc.

Guichard, F., Redelsperger,J.-L. and Lafore, J.-P. (1996) The behaviour of a cloud ensemble in response to external forcings, Q.J.R.M.Soc., 122, 1043-1074

Holland, J.Z. and Rasmusson, E.M. 1973 Measurements of atmospheric mass, energy and momentum budgets over a 500-kilometer square of tropical ocean, Mon. Wea. Rev., 101, 44-55

Kain, J.S. and Fritsch, J.M. (1990) A one-dimensional entraining/detraining plume model and its application to convective parametrization, J. Atm. Sci., 47, 2784-2802

Kershaw, R. and Gregory, D. (1997) Parametrization of momentum transports by convection. I: Theory and cloud modelling results, Accepted for publication in QJR. Meteorol. Soc.

Moorthi, S. and Suarez, M.J. (1992) Relaxed Arakawa-Schubert : a parametrization of moist convection for general circulation models, Mon. Wea. Rev., 120, 978-1002

Nordeng, T.E. (1994) Extended versions of the convection parametrization scheme at ECMWF and their impact upon the mean climate and transient activity of the model in the tropics, Research Department Technical Memorandum No. 206, ECMWF, Shinfield Park, Reading, Berks, United Kingdom

Ooyama, K. (1971) A theory on parametrization of cumulus convection, J. Met. Soc. Jap., 49 (Special Issue), 744-756

Raymond, D.J. (1995) Regulation of moist convection over the west Pacific warm pool, J. Atm. Sci., 52, 3945-3959

Raymond, D.J. and Blyth, A.M. (1986) A stochastic mixing model for non-precipitating cumulus clouds, J. Atm. Sci., 43, 2708-2718

Siebesma, A.P. and Holtslag, A.A.M. (1996) Model impacts of entrainment and detrainment rates in shallow cumulus convection, J. Atm. Sci., 53, 2354-2364

Slingo, J.M., Sperber, K.R., Boyle, J.S., Ceron, J.-P., Dix, M., Dugas, B., Ebisuzaki, W., Fyfe, J., Gregory, D., Gueremy, J.-F., Hack, J., Harzallah, A., Inness, P., Kitoh, A., Lau, W.K.-M., McAvaney, B., Madden, R., Matthews, A., Palmer, T.N., Park, C.-K., Randall, D. and Renno, N. (1996) Intraseasonal oscillations in 15 atmospheric general circulation models : results from an AMIP diagnostic subproject, Clim. Dyn. 12, 325-357

Soong, S.-T. and Ogura, Y. (1980) Response of trade wind cumuli to large-scale processes, J. Atm. Sci., 37, 2035-2050

Spencer, R.W. (1993) Global oceanic precipitation from MSU during 1979-91 and comparison to other climatologies, J. Clim., 6, 1301-1326

Tiedtke, M. (1989) A comprehensive mass flux scheme for cumulus parametrization in large-scale models, Mon. Wea. Rev., 117, 1779-1800

Yanai, M., Esbensen, S. and Chu, J-H. (1973) Determination of bulk properties of tropical cloud clusters from large-scale heat and moisture budgets, J. Atm. Sci., 30, 611-627

Yao, M.-S. and DelGenio, A.D. (1989) Effects of cumulus entrainment and multiple cloud types on a January global climate model simulation, J. Clim., 2, 850-863